FORWARD AND REVERSE EXCITATION ENERGY TRANSPORT MONITORED BY MONTE - CARLO SIMULATIONS

LESZEK KUŁAK[1] and PIOTR BOJARSKI[2]

[1] *Department of Technical Physics and Applied Mathematics, Technical University of Gdańsk, Narutowicza 11/12, 80-952 Gdańsk, Poland*
kulak@pg.gda.pl
[2] *University of Gdańsk, Institute of Experimental Physics, Luminescence Research Group, Gdańsk, ul. Wita Stwosza 57, 80-952 Gdańsk, Poland.*

Abstract: Monte Carlo study of nonradiative excitation energy transport in binary disordered systems is presented. Two methods of simulations are employed and tested. The results for emission anisotropy, quantum yield and fluorescence decay are compared with those of self-consistent diagrammatic model (SCDM).

I. Introduction

Nonradiative excitation energy transport (NEET) in disordered systems has been a subject of intensive theoretical and experimental studies for several decades [1,2]. The reason is not only still remaining strong interest in this phenomenon, but first of all its numerous applications in different areas of science and technology. The NEET process occurs in various biological systems, plays a very important role in photosynthesis, photographic industry, affects the parameters of dye lasers to name only a few.

Recently, rapid progress has been made in the theoretical treatment of the NEET in binary donor - acceptor systems by taking into account not only forward (D* → D, D* → A), but also reverse nonradiative energy transport (RNET) (A* → A, A* → D) [3-8]. Theoretical investigations of this latter process have been carried out within the frameworks of so called hopping [3-5] and diagrammatic models [6-8]. The hopping model, though quite straightforward in practical applications seems to be mostly oversimplified. The diagrammatic model represents a more systematic approach and its results are more general than those predicted by other theories.

By now, only several experimental papers dealing with comparison to analytical theories are known [9-11]. The reason is not only the novelty of the RNET pheno-menon, but also serious experimental difficulties concerning selection of appropriate

systems in which the "pure" effect can be observed as well as the demand for high sensitivity of the experimental setup.

Having this in mind, Monte - Carlo simulation seems to be a perfect tool to gain profound insight into the mechanism of the RNET. Specifically, the consistency of any NEET theory can be verified and possible reasons responsible for disagreement between the theory and experiment can easier be identified.

The aim of this paper is to fill partly this gap and to provide more information on the mechanism of the RNET through the Monte-Carlo simulation (MC) method. Two different MC techniques will be presented in detail and evaluated. A comparison of the MC results to those of the SCDM will be presented.

II. The master equation and Green function

In this paper we will restrict the theoretical part only to the necessary considerations required for comparison with the results of Monte Carlo simulations. Let us consider a system of volume Ω in which energy can be transferred incoherently between N donors (D) and M acceptors (traps) (A) randomly distributed with number density ρ_D and ρ_A, respectively. Each molecular configuration $\mathfrak{R}$ of the system is characterized by the locations $(r_1, r_2, ..., r_{N+M})$ of the molecules. The donor molecules are labelled 1 through N, and the acceptor molecules N+1 through N+M. The probability that the excitation is on the j-th molecule at time t, $p_j(t)$, for the fixed molecular configuration obeys the following *master equation* [6]:

$$\frac{dp_j}{dt} = \sum_{k=1,j\neq k}^{N} w_{jk}^{DD}p_k - \sum_{k=1,j\neq k}^{N} w_{kj}^{DD}p_j - \sum_{k=N+1}^{N+M} w_{kj}^{DA}p_j + \sum_{k=N+1}^{N+M} w_{jk}^{AD}p_k - p_j/\tau_{oD}, \quad 1 \leq j \leq N.$$

(1)

$$\frac{dp_j}{dt} = \sum_{k=1}^{N} w_{jk}^{DA}p_k - \sum_{k=1}^{N} w_{kj}^{AD}p_j + \sum_{k=N+1,j\neq k}^{N+M} w_{jk}^{AA}p_k - \sum_{k=N+1,j\neq k}^{N+M} w_{kj}^{AA}p_j - p_j/\tau_{oA}, \quad N+1 \leq j \leq N+M.$$

The distance dependent transfer rate from the *j*-th X molecule to the *i*-th Y molecule $((x,y \in \{D,A\})$ is denoted by w_{ij}^{XY} (w_{ii}^{XY} is defined to be zero). τ_{oD} and τ_{oA} are the lifetimes of donor and acceptor molecules, respectively, measured in the absence of the intermolecular transfer. For the sake of simplicity we shall assume the absence of the diagonal disorder. Under this assumption, the transfer rates $w_{ij}^{XX} = w_{ji}^{XX}$, $x \in \{D,A\}$ are symmetric. The coherence and volume effects are also neglected.

Master equation in the compact matrix notation can be given by:

$$\frac{dP(\mathfrak{R}, t)}{dt} = W \circ P(\mathfrak{R}, t),$$

(2)

where $P(\mathfrak{R},t)$ is a vector with components $p_1(t)$, $p_2(t)$, ..., $p_{N+M}(t)$ and W is the N+M matrix defined as:

$$W_{jk} = w_{jk}^{DD} - \delta_{jk}\left[\sum_{i=1}^{N} w_{ik}^{DD} + \sum_{i=N+1}^{N+M} w_{ik}^{DA} - 1/\tau_{0D}\right], \quad j \leq N, \ k \leq N,$$

$$W_{jk} = w_{jk}^{DA}, \quad N+1 \leq j \leq N, \ k \leq N,$$

$$W_{jk} = w_{jk}^{AD}, \quad j \leq N, \ N+1 \leq k \leq N+M, \tag{3}$$

$$W_{jk} = w_{jk}^{AA} - \delta_{jk}\left[\sum_{i=1}^{N} w_{ik}^{AD} + \sum_{i=N+1}^{N+M} w_{ik}^{AA} - 1/\tau_{0A}\right], \quad j \geq N+1, \ k \geq N+1.$$

In the case of the dipole-dipole interaction the transfer rate is given by :

$$w_{ij}^{XY} = \frac{1}{\tau_{0X}}\left(\frac{R_0^{XY}}{r_{ij}}\right)^6, \quad X, Y \in \{D, A\}, \tag{4}$$

and τ_{0X} denotes the actual lifetime of X molecule for the concentration of Y molecules $\rho_Y \to 0$, R_0^{XY} denotes the critical radius for the energy transfer which can be determined from the experimental data.

Information concerning the excitation energy transport in the system considered can be obtained from the time and distance-dependent ensemble averaged density of excitations:

$$\mathcal{P}(\mathbf{r}, t) = \left\langle \sum_{j=1}^{N+M} \delta(\mathbf{r}_j - \mathbf{r}) p_j(\mathfrak{R}, t) \right\rangle \equiv \frac{1}{\Omega^{N+M}}\int d\mathbf{r}_1 \cdots \int d\mathbf{r}_{N+M} \sum_{j=1}^{N+M} \delta(\mathbf{r}_j - \mathbf{r}) p_j(\mathfrak{R}, t). \tag{5}$$

The solution to Eq. (2) can be expressed using the Green function [6-8,12,13], $\mathcal{G}(\mathbf{r}, \mathbf{r}', t)$, defined by the following relation:

$$\mathcal{P}(\mathbf{r}, t) = \int d\mathbf{r}' \, \mathcal{G}(\mathbf{r}, \mathbf{r}', t) \mathcal{P}(\mathbf{r}', 0). \tag{6}$$

or it can be obtained from the Monte Carlo simulation.

If the initial probability distribution function is determined by the spatial distribution of the excitation pulse, and if we assume that no acceptors are excited at time $t = 0$, then the Green function is given by:

$$\mathcal{G}(\mathbf{r}, \mathbf{r}', t) = \frac{\Omega}{N} \sum_{j=1}^{N+M} \sum_{k=1}^{N} \left\langle \delta(\mathbf{r}_j - \mathbf{r})\delta(\mathbf{r}_k - \mathbf{r}')(\exp(t\,W))_{jk} \right\rangle. \tag{7}$$

The Green function has the physical meaning of the averaged conditional probability density of the excitation being found at a position $\mathbf{r}$ at a time t, if it has been created at the initial time moment $(t = 0)$ at the origin $\mathbf{r}'$.

The Green function can be portioned into the diagonal part $\mathscr{G}^{SD}(\mathbf{r},\mathbf{r}',t)$, which represents the density of the initial site survival probability (it can be measured in the fluorescence depolarization experiment), and the non-diagonal parts, $\mathscr{G}^{DD}(\mathbf{r},\mathbf{r}',t)$ and $\mathscr{G}^{DA}(\mathbf{r},\mathbf{r}',t)$, representing the probability densities of the excitation being found on a donor other than the initially excited one, and on an acceptor, respectively (they are related to the mean square displacement and to the decay function).

$$\mathscr{G}(\mathbf{r},\mathbf{r}',t) = \mathscr{G}^{SD}(\mathbf{r},\mathbf{r}',t) + \mathscr{G}^{DD}(\mathbf{r},\mathbf{r}',t) + \mathscr{G}^{DA}(\mathbf{r},\mathbf{r}',t) , \tag{8}$$

where

$$\mathscr{G}^{SD}(\mathbf{r},\mathbf{r}',t) = \delta(\mathbf{r} - \mathbf{r}')\big\langle(\exp(t\,W))_{11}\big\rangle , \tag{9}$$

$$\mathscr{G}^{DD}(\mathbf{r},\mathbf{r}',t) = (N-1)\big\langle\delta(\mathbf{r}_{12} - \mathbf{r} + \mathbf{r}')(\exp(t\,W))_{21}\big\rangle , \tag{10}$$

$$\mathscr{G}^{DA}(\mathbf{r},\mathbf{r}',t) = M\big\langle\delta(\mathbf{r}_{1,N+1} - \mathbf{r} + \mathbf{r}')(\exp(t\,W))_{N+1,1}\big\rangle . \tag{11}$$

To take into account the reverse excitation energy transfer the Green functions $\mathscr{G}^{SA}(\mathbf{r},\mathbf{r}',t)$, $\mathscr{G}^{AA}(\mathbf{r},\mathbf{r}',t)$ and $\mathscr{G}^{AD}(\mathbf{r},\mathbf{r}',t)$ should additionally be introduced. This is in connection with the process of energy transfer in the presence of energy migration in the acceptor ensemble.

III. Fluorescence observables

The nature of energy transport at long times and high concentrations can conveniently be investigated by performing the Fourier-Laplace transform of the Green function $\mathscr{G}(\mathbf{r},\mathbf{r}',t)$:

$$\hat{\mathscr{G}}(\mathbf{k},\varepsilon) = \int_0^\infty dt\,\exp(-\varepsilon t)\int_{R^3} d|\mathbf{r} - \mathbf{r}'|\exp(i\,\mathbf{k}\,|\mathbf{r} - \mathbf{r}'|)\mathscr{G}(|\mathbf{r} - \mathbf{r}'|,t) \tag{12}$$

If we define the quantity:

$$\hat{\mathscr{G}}^{D}(\mathbf{k},\varepsilon) = \hat{\mathscr{G}}^{SD}(\varepsilon) + \hat{\mathscr{G}}^{DD}(\mathbf{k},\varepsilon) \tag{13}$$

as the Fourier-Laplace transform of the probability density that the excitation is being found in the donor ensemble, then by inverting it for $\mathbf{k} = 0$:

$$\Phi_D(t) = \mathscr{L}_t^{-1}\big(\hat{\mathscr{G}}^{D}(\mathbf{k} = 0,\varepsilon)\big), \tag{14}$$

we obtain the donor fluorescence decay $\Phi_D(t)$. In other words, *the fluorescence decay curve describes the relative number of excited donor molecules at time t after excitation.*

Moreover, the function $\hat{\mathcal{G}}^D(\mathbf{k}, \varepsilon)$ is strictly connected with the steady-state fluorescence observables, like, the relative quantum yield and the emission anisotropy. The donor relative quantum yield, η_D/η_{0D}, *the ratio of emitted and absorbed quanta by donors,* can be expressed as:

$$\eta_D / \eta_{0D} = (1 / \tau_{0D}) \hat{\mathcal{G}}^D(\mathbf{k} = 0, \varepsilon = 0) \tag{15}$$

and the relative quantum yield of initially excited donors:

$$\eta_i / \eta_{0D} = (1 / \tau_{0D}) \hat{\mathcal{G}}^{SD}(\varepsilon = 0). \tag{16}$$

If a sample of randomly oriented molecule is excited by a short pulse of linearly polarized light, the emission anisotropy of observed light can be written as

$$r(t) = \frac{I_{\Pi}(t) - I_{\perp}(t)}{I_{\Pi}(t) + 2I_{\perp}(t)}, \tag{17}$$

where $I_{\Pi}(t)$ and $I_{\perp}(t)$ denote the paralell and perpendicular fluorescence intensity components to the direction of the polarization vector of the exciting pulse, respectively. The fluorescence emission anisotropy can be calculated from the relation:

$$r_D / r_{0D} = \eta_i / \eta_D \tag{18}$$

which can be very easy exploited in the Monte Carlo simulations.

If we write out the formulas for Fourier-Laplace transform of the investigated Green functions $\hat{\mathcal{G}}^{XY}(\mathbf{k}, \varepsilon)$ $X, Y \in \{D, A\}$ explicitly, then a series of products of w_{ij}^{XY} factors is obtained. Next, to determine the resulting Green functions, we have to sum up all of these products ($n \rightarrow \infty$). An excellent tool for this purpose is the diagrammatic technique [3,4,10-12].

As it was shown in our previous paper [11] the Green functions $\hat{\mathcal{G}}^{DD}(\mathbf{k}, \varepsilon)$ in the $\mathbf{k} = 0$ limit fulfill the following self-consistent equation:

$$(\varepsilon + 1 / \tau_{0D})[\hat{\mathcal{G}}^{SD}(\varepsilon) + \hat{\mathcal{G}}^{DD}(\mathbf{k} = 0, \varepsilon)] + (\varepsilon + 1 / \tau_{0A})\hat{\mathcal{G}}^{DA}(\mathbf{k} = 0, \varepsilon) = 1 \tag{19}$$

Substituting the explicit formulas of the Green functions $\hat{\mathscr{G}}^{XY}$, $X,Y \in \{D,A\}$ into Eq.(19) leads to the following equations:

$$\left(\hat{\mathscr{G}}^{SX} - \frac{1}{\varepsilon_X} + \frac{\hat{\Sigma}^{XX}}{\rho_X \varepsilon_X \hat{\mathscr{G}}^{SX}}\right)\left(1 - \frac{\hat{\Sigma}^{YY}}{\rho_Y \hat{\mathscr{G}}^{SY}}\right) + \frac{\varepsilon_Y \hat{\Sigma}^{XY}}{\varepsilon_X \rho_X}\left(1 + \frac{\hat{\Sigma}^{YX}}{\varepsilon_Y \rho_Y \hat{\mathscr{G}}^{SX}\hat{\mathscr{G}}^{SY}}\right) = 0, \quad X,Y \in \{D,A\} \quad (20)$$

Equation (20) is the basis for the self-consistent approximation procedure applied to the fluorescence observables. Let us review the consecutive steps of this procedure. $\hat{\mathscr{G}}^{SD}(\varepsilon)$ and $\hat{\mathscr{G}}^{SA}(\varepsilon)$ are assumed to be the unknown functions. Next, we partially sum the diagrammatic series for functions $\hat{\Sigma}^{XY}$, $X,Y \in \{D,A\}$. When these approximations are inserted into coupled nonlinear Eq.(20), the resulting equations involve only unknown functions $\hat{\mathscr{G}}^{SD}(\varepsilon)$ and $\hat{\mathscr{G}}^{SA}(\varepsilon)$ and they can be solved. Then after substituting these solutions into the partially summed series for $\hat{\Sigma}^{XY}$ one finally obtains the expressions for the considered Green functions $\hat{\mathscr{G}}^{XY}$.

The function $\hat{\mathscr{G}}^{D}(k, \varepsilon)$ can be calculated from Eq.(13) using Eq.(20) with the result:

$$\hat{\mathscr{G}}^{D} = \frac{\hat{\mathscr{G}}^{SD}}{1 - \dfrac{\hat{\Sigma}^{DD}}{\rho_D \hat{\mathscr{G}}^{SD}} - \dfrac{\hat{\Sigma}^{DA}\hat{\Sigma}^{AD}}{\rho_D \rho_A \hat{\mathscr{G}}^{SD}\hat{\mathscr{G}}^{SA}\left(1 - \hat{\Sigma}^{AA}/\rho_A\hat{\mathscr{G}}^{SA}\right)}}. \quad (21)$$

This equation enables to obtain the donor fluorescence decay by its numerical invertion.

Moreover, by inserting the explicit form [11-12] of the Green functions $\hat{\mathscr{G}}^{XY}$ into Eqs.(15) and (18) (versus the variables $\hat{\Sigma}^{XY}$, $\hat{\mathscr{G}}^{SD}(\varepsilon)$ and $\hat{\mathscr{G}}^{SA}(\varepsilon)$) we obtain:

$$\eta_D / \eta_{0D} = \frac{1}{1 + \dfrac{\tau_{0D}\,\hat{\Sigma}^{DA}/\tau_{0A}\rho_D}{\hat{\mathscr{G}}^{SD}\left(1 - \hat{\Sigma}^{AA}/\rho_A\hat{\mathscr{G}}^{SA}\right)}}, \quad \varepsilon = 0 \quad (22)$$

and

$$r_D / r_{0D} = 1 - \frac{\hat{\Sigma}^{DD}}{\rho_D \hat{\mathscr{G}}^{SD}} - \frac{\hat{\Sigma}^{DA}\hat{\Sigma}^{AD}}{\rho_D \rho_A \hat{\mathscr{G}}^{SD}\hat{\mathscr{G}}^{SA}\left(1 - \hat{\Sigma}^{AA}/\rho_A\hat{\mathscr{G}}^{SA}\right)}, \quad \varepsilon = 0. \quad (23)$$

(r_{0D} is the donor emission anisotropy, when $\rho_A \to 0$; $\hat{\Sigma}^{XY}$ are the diagrammatic series appearing in the definition of the Green functions $\hat{\mathscr{G}}^{XY}(k, \varepsilon)$).

One can see from Eq.(23) that in the presence of the RNEET the emission anisotropy decreases due to the excitation energy transfer from the excited acceptors to unexcited donors ($\hat{\Sigma}^{AD} \neq 0$). In the presence of the energy migration in the acceptor

ensemble ($\hat{\Sigma}^{AA} \neq 0$), a decrease in the relative donor quantum yield and emission anisotropy is expected.

The formulas for fluorescence observables presented above form our theoretical basis for the so-called self-consistent diagrammatic model (SCDM), predictions of which will be compared to the results of Monte Carlo simulations.

IV. Monte Carlo simulation of the donor fluorescence obserwables

In a simulation, N donors of concentration C_D and M acceptors of concentration C_A, are randomly distributed in a three-dimensional cube (C_X is the number of molecules X in volume Ω). The dynamics of the system considered is described by Eq.(1). The effect of the finite size of generated system is reduced by introducing periodic boundary conditions (the cube is surrounded by replicas of itself) with minimum image convention (the molecule interacts with another molecule or with its periodic image).

The concentration course of the quantities of interest is obtained by rescaling critical radii for energy transfer and keeping the length of the cube edge equal to 1. The pseudo-random number generator (mixed congruential generator with the period of 2^{32}), which passed several statistical tests was also verified by checking the simulated statistical clusters concentration against the analytically expected value.

The simulated configurations were sampled until the relative variance of the luminescent observables attained less then 0.1 %.

IV.1.Steady-state obserwables

The formal solution to Eq.(2) is

$$P(t) = \exp(t\,W) \circ P(t = 0) \tag{24}$$

The matrix $\mathscr{G}(t) = \exp(t\,W)$ is the Green function which elements $g_{ij}(t)$ are conditional probabilities that the *i-th* molecule is excited at time t if at time t=0 the *j-th* molecule was excited.

Asymptotic behaviour (steady-state values) of such observables as quantum yield and fluorescence anisotropy can be conveniently monitored performing the Laplace transform of matrix $\exp(t\,W)$. The resulting matrix $\mathscr{L}_\varepsilon(\mathscr{G}(t)) = (\varepsilon I + W)^{-1}$ for $\varepsilon = 1 / \tau_{0D}$, leads to the following expressions for steady state observables:

$$r_D / r_{0D} = \left\langle \sum_{i}^{N}\left[\left(I + \tau_{0D}W\right)^{-1}\right]_{ii} / \sum_{i,j}^{N}\left[\left(I + \tau_{0D}W\right)^{-1}\right]_{ij} \right\rangle, \tag{25}$$

$$\eta_D / \eta_{0D} = \left\langle \sum_{i,j}^{N}\left[\left(I + \tau_{0D}W\right)^{-1}\right]_{ij} \right\rangle / N , \tag{26}$$

where the symbol $< ... >$ denotes the average over all possible configurations of molecules, I is an identity matrix. The inverse matrix of $I + \tau_{0D} W$ cannot be calculated analytically, but it can be exploited very well in the Monte-Carlo simulation. The matrix $I + \tau_{0D} W$ is not symmetric and it is defined as positive. This non-symmetric matrice was inverted by the Gauss procedure which was tested to show whether a system with no acceptors gives a quantum yield equal to unity. For N up to 600, the observed deviations were very small for all experimentally accessible concentrations (maximal error less then 0.01 %). Then, after a suitable number of simulated runs, averaged quantities of interest are calculated. The number of molecules N for individual simulation runs is limited by the CPU time consumption and numerical stability. After performing several convergence tests, N = 500 was chosen as a sufficient number of molecules. The number of necessary simulated configurations depends on molecular concentration. Therefore, at low concentrations smaller number of runs were sampled (e.g. 5000) than for intermediate concentrations. At very high concentrations, because of a strong dependence of the emission anisotropy on the number of molecules, much more runs with higher number of molecules is indispensable.

When applying the method of inverting relaxation matrix, the steady-state obserwables depend on the number of molecules N. This dependence is especially strong in the case of one-component system, as it is illustrated in Figure 1. For very high donor reduced density the relative emission anisotropy tends to the value 1/N. Therefore, to avoid this error one should perform Monte Carlo run with the number of molecules as high as possible. Of course, the CPU time consumption stands as a barrier for increasing N. Fortunately, a careful analysis of one-component system leads to the conclusion that the correct values of emission anisotropy can be obtained throughout the whole density range, if the limiting value 1/N is subtracted from the simulated values obtained in the Monte Carlo simulation for a given N [19]. For two-component system strong dependence of luminescent observables on N is not observed. Compared to other Monte Carlo techniques this method is very efficient for one component system and for small acceptor concentrations in the case of two-component system. The time of individual simulation run increases with N^3, where N is the number of molecules in the simulation.
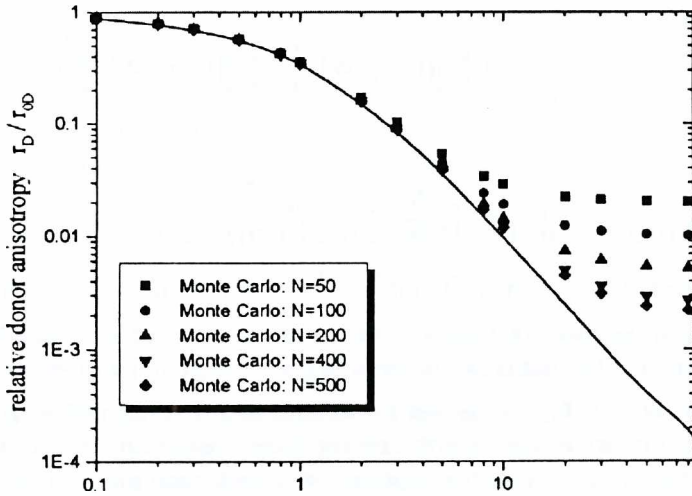
Fig. 1. Donor fluorescence emission anisotropy r_D / r_{0D} versus the reduced donor concentration, γ_D, for one component system. Solid curve represents the theoretical results [2]. Squares (■), full circles (●), up triangles (▲), down triangles (▼) and diamonds (♦), denote the results of the Monte Carlo simulation for different number of molecules in the system, respectively. As seen from the figure the relative donor emission anisotropy decreases with concentration. This is due to the fact that energy migration increases with molecular concentration which diminishes the probability of fluorescence emission by primarily excited donor (see also Eq.18).

IV.2. Step by step Monte Carlo method

The "step by step" Monte Carlo simulation method [14,15] consists in the employment of the random-number generator for the cyclic formulation of answers to two questions: when any of the preset luminescent processes will take place in the simulated system, and what kind of process it will be. This method was applied to investigate such phenomena as the concentration depolarization of fluorescence , the quantum yield and the shape of the decay curves.

The simulation algorithm include the following steps:

1^0 the coordinates of a primarily excited molecule are determined (using random number generator). This molecule can be deactivated through the following processes:

(P$_1$) process 1: $D^* \rightarrow D$, photon emission or nonradiative energy conversion, with the rate $1 / \tau_{0D}$;

(P$_2$) process 2: $D^* + D \rightarrow D + D^*$, energy migration (energy transfer to the molecules of the same kind), with the transfer rate w_{ij}^{DD};

(P3) process 3: $D^* + A \rightarrow D + A^*$ nonradiative energy transfer from the excited donor to an acceptor, with the transfer rate w_{ij}^{DA};

2^0 If i-th donor molecule is excited, the values of the following total transfer rates

$$c_{1i} = 1/\tau_{0D}, \qquad c_{2i} = \sum_{j=1, i \neq j}^{N} w_{ji}^{DD}, \qquad c_{3i} = \sum_{j=N+1}^{N+M} w_{ji}^{DA} \qquad (27)$$

have to be calculated. Otherwise, when i-th acceptor is excited, the values of:

$$c'_{1i} = 1/\tau_{0A}, \qquad c'_{2i} = \sum_{j=N+1, i \neq j}^{N+M} w_{ji}^{AA}, \qquad c'_{3i} = \sum_{j=1}^{N} w_{ji}^{AD} \qquad (28)$$

are calculated.

3^0 The time at which any of the investigated processes occur (cp. step 1^0) is calculated by inverting the distribution function of the probability, $p_i(t, P_k)dt$, that if at time t the i-th molecule is excited, then the process P_k appears in the time interval (t, t+dt):

$$p_i(t) = \sum_{k=1}^{3} p(t, P_k) = c_i \exp(-c_i t) \qquad (29)$$

where

$$c_i = c_{1i} + c_{2i} + c_{3i} \qquad (30)$$

For this purpose a random number r_{1i} is generated and the time at which any process takes place is obtained by inverting the distribution function of the probability $p_i(t, P_k)$,

$$\int_0^{t_i} p_i(t)dt = r_{1i}, \text{ i.e. } t_i = -(1/a_i)\ln r_{1i} \qquad (31)$$

The same procedure can be applied to the excited acceptor. In this case all constants c_{ji} should be replaced by c'_{ji}, $j = 1,2,3$

4^0 In this step it is determined which process took place at time t_i. By generating next random number, r_{2i}, such a value of index k can be found for which the following inequality is satisfied:

$$\sum_{j=1}^{k-1} c_{ji} < r_{2i} c_i \leq \sum_{j=1}^{k} c_{ji}, k = 1,2,3 \qquad (32)$$

If k=1, then the activated molecule is quenched by a photon emission or nonradiative excitation energy conversion and it means that this pass of simulation is finished. If k=2 or k=3, the energy migration or energy transfer process takes place,

and it is necessary to determine which molecule will be now activated. For this reason the third random number, r_{3i} is generated and the value of index n is found which fulfill one of the inequalities:

$$\sum_{j=1}^{n-1} w_{ji}^{DD} < r_{3i}\left(c_{1i} + c_{3i}\right) \le \sum_{j=1}^{n} w_{ji}^{DD}, \text{for } n \le N \tag{33}$$

or

$$\sum_{j=1}^{N} w_{ji}^{DD} + \sum_{j=N+1}^{n-1} w_{ji}^{DA} < r_{3i}\left(c_{1i} + c_{3i}\right) \le \sum_{j=1}^{N} w_{ji}^{DD} + \sum_{j=N+1}^{n} w_{ji}^{DA}, \text{for } n > N \tag{34}$$

where n is the number of next activated donor or acceptor molecule. Then, after inserting the value of n for the index i, the simulation goes to step 2^0. The simulation run is finished when after several migration or transfer energy acts the process with k=1 occurs in step 4^0 (photon emission or nonradiative energy conversion). After that new simulation can run (i.e. for a new donor and acceptor spatial configuration).

In the case when an acceptor is excited, the number of the next excited molecule ,n, is determined from the relations:

$$\sum_{j=N+1}^{n-1} w_{ji}^{AA} < r_{3i}\left(c'_{1i} + c'_{3i}\right) \le \sum_{j=N+1}^{n} w_{ji}^{AA}, \text{for } n \le N+M \tag{35}$$

and

$$\sum_{j=N+1}^{N+M} w_{ji}^{AA} + \sum_{j=1}^{n-1} w_{ji}^{AD} < r_{3i}\left(c'_{1i} + c'_{3i}\right) \le \sum_{j=N+1}^{N+M} w_{ji}^{AA} + \sum_{j=1}^{n} w_{ji}^{AD}, \text{for } n < N \tag{36}$$

The relative donor quantum yield is calculated by dividing the number of simulation runs finished with the donor emission by the number of all runs. The relative donor emission anisotropy is calculated from the relation $r_D / r_{0D} = \eta_i / \eta_D$, where η_i is the quantum yield of initially excited donors and η_D is the total donor quantum yield, i.e., dividing the number of simulation runs finished with primarily excited donor emission by the total number of runs.

The donor decay curve is obtained in a way similar to the real experiment, i.e., the time scale (e.g. $[0, 3\ \tau_{0D}]$) is divided into appropriate number of intervals (e.g. 2048) and, if photon emission at the time t_i is "observed", then the number of photons is increased in the respective "channel". Finally, the normalized decay curve (histogram) is obtained using a simple formula:

$$\Phi_D\left(\Delta t_k\right) = 1 - \left(\sum_{j=1}^{k} n_j / \sum_{j=1}^{k_{max}} n_j\right), \qquad \Delta t_k = \left(k / k_{max}\right)t \tag{37}$$

where n_k denotes the number of photons in the k-th channel, k_{max} is the total number of all channels.

The steady-state values of relative emission anisotropy for the system of rhodamine 6G (donor) and rhodamine B (acceptor) in glycerol solution obtained using the "step by step" Monte Carlo simulation are presented in Figure 2.
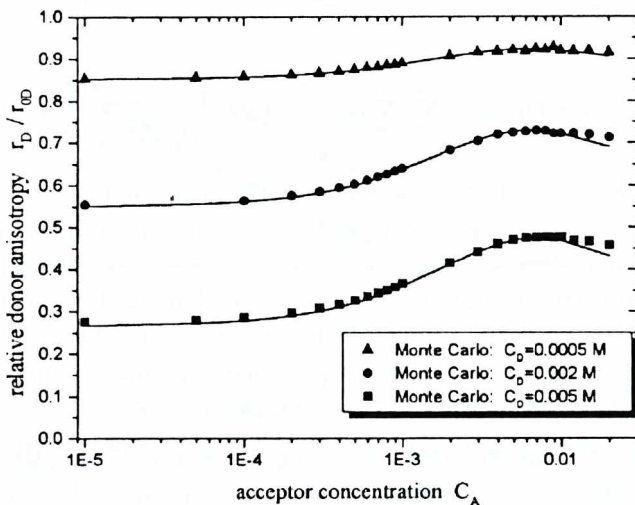
Fig. 2. Donor fluorescence emission anisotropy r_D / r_{0D} versus the acceptor concentration. C_A, at fixed donor concentration in the presence of forward and reverse energy transfer. Solid theoretical curves are calculated in the framework of the SCDM model [11,12]. Triangles (▲), full circles (●) and squares (■) denote the results of the Monte Carlo simulation.

Figure 2 shows the results obtained for low and high donor concentrations. Simulation data for the emission anisotropy were obtained for different acceptor concentrations at fixed concentration of the donor. Theoretical curves are denoted by solid lines; full circles and squares and triangles denote the results of the Monte Carlo simulation. As seen the theoretical curves are in a very good agreement with the results of Monte Carlo simulation nearly for all the acceptor concentrations, which indicates the consistency of the SCDM method.

The step-by-step Monte Carlo method is generally a very efficient and complete method and it can be applied to a wide variety of investigated systems. The CPU time consumption necessary for a simulation run is lower then in other methods.

IV.3. Monte Carlo simulation of the donor fluorescence decay

The fluorescence decay profile $\Phi_D(t)$ can be described in terms of eigenvectors and eigenvalues [16-18] in the following way:

Let us assume that the matrix D is the diagonal matrix the main diagonal of which contains the eigenvalues of matrix W and that matrix Z is the matrix of right eigenvectors of matrix W. In matrix Z, the eigenvector corresponding to the

eigenvalue λ_i is located in the *i-th* column of matrix Z. Thus, the donor and acceptor fluorescence decay profile are given by

$$\Phi_D(t) = k_{FD}\sum_{i=1}^{N}p_i(t) = k_{FD}\sum_{i=1}^{N}\sum_{j=1}^{N+M}\left(e^{tW}\right)_{ij}p_j(0) = \frac{k_{FD}}{N}\sum_{i=1}^{N}\sum_{j=1}^{N}\sum_{k=1}^{N+M}\left(Z^{-1}\right)_{ik}Z_{kj}\,e^{-\lambda_k t}\,, \quad (38)$$

$$\Phi_A(t) = k_{FA}\sum_{i=N+1}^{N+M}p_i(t) = k_{FA}\sum_{i=N+1}^{N+M}\sum_{j=1}^{N+M}\left(e^{tW}\right)_{ij}p_j(0) = \frac{k_{FA}}{N}\sum_{i=N+1}^{N+M}\sum_{j=1}^{N}\sum_{k=1}^{N+M}\left(Z^{-1}\right)_{ik}Z_{kj}\,e^{-\lambda_k t} \quad (39)$$

where k_{FD} and k_{FA} are the rate constants for the donor and acceptor fluorescence, respectively. The eigenvectors and eigenvalues of real nonsymmetric matrix W were computed as follows: first, the matrix was balanced; second, accumulating orthogonal similarity transformations were used to reduce the balanced matrix to a real upper Hessenberg matrix; third, the shifted QR algorithm was used to compute the eigenvectors and eigenvalues of this Hessenberg matrix. The inverse matrix to matrix Z was calculated using the standard numerical Gauss procedure.

The fluorescence acceptor and donor decay profiles $\Phi_A(t)$, $\Phi_D(t)$ obtained in terms of eigenvectors and eigenvalues of the relaxation matrix W for two-component system are presented in the Figures 3 and 4, respectively.
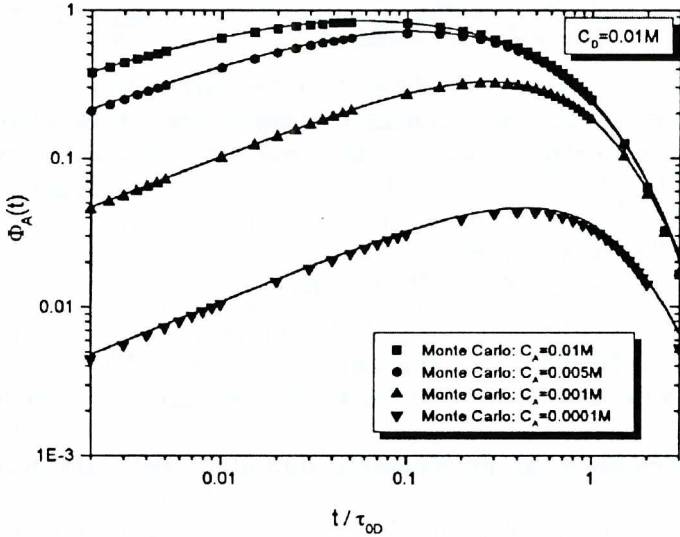
Fig. 3. Acceptor fluorescence decay $\Phi_A(t)$, versus the time t, at fixed donor concentration for various acceptor concentration in the presence of forward and reverse energy transfer. Solid theoretical curves are calculated in the framework of the SCDM model [11,12]. Full circles (●), squares (■), triangles up(▲) and down (▼), denote the results of the Monte Carlo simulation.
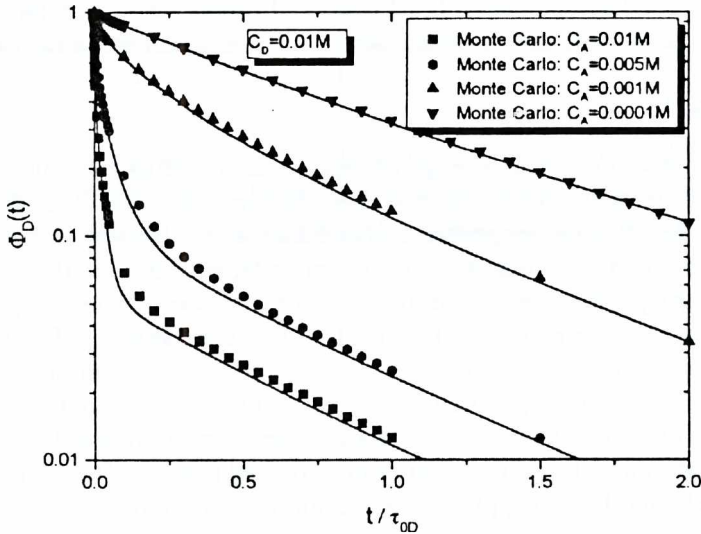
Fig. 4. Donor fluorescence decay $\Phi_D(t)$ versus the time t, at fixed donor concentration for various acceptor concentrations in the presence of forward and reverse energy transfer. Solid theoretical curves are calculated in the framework of the SCDM model [11,12]. Full circles (●), squares (■), triangles up (▲) and down (▼), denote the results of the Monte Carlo simulation.

Figure 3 shows the acceptor fluorescence decay obtained for high fixed donor and several acceptor concentrations. This figure is particularly interesting, since it is not possible to measure directly the acceptor fluorescence observables in the experiment of interest. It is seen from the figure that shortly after pulse excitation the number of fluorescing acceptors increases, then attains its maximum followed by a rapid depopulation of the excited state. Such a character of this temporal course is determined by the relation between the effective rate of energy transfer between donor and acceptor species and the rate of spontaneous emission and differs visibly from that of donors. The reason is that at time t=0 there are no excited acceptors, but only donors which absorb the excitation energy. At times t > 0 acceptors receive nonradiatively the excitation energy from donors and their number in the excited state increases. From now on they start to emit fluorescence and return the excitation energy to the donor ensemble. These donors can either emit fluorescence or transfer the excitation energy again to the acceptor set. These processes can repeat an arbitrary number of times. The correctness of the decay kinetics predicted by the SCDM is confirmed by the MC results.

Figure 4 shows the donor fluorescence decays obtained for the same systems. The monotoneous character of the donor decay can be seen in this figure. It results from the fact that at t=0 donors are excited by the pulse of light (acceptors are unexcited) and from now on the depopulation of their excited state starts either through the fluorescence or nonradiative transfer to acceptors, the latter process being somewhat slowed down by the back transfer to the donors. As seen theoretical curves

are in a very good agreement with the results of Monte Carlo simulation nearly for all the acceptor concentrations, which again confirms the consistency of the SCDM.

Final remarks

Nonradiative excitation energy transport was investigated using two different MC methods, namely step by step and relaxation matrix method. Both methods equally well describe the properties energy transport and the agreement between the SCDM theory and MC results is excellent independently of the method used. However, step by step method is straightforward and more efficient, especially in the case of complex systems due to lower CPU time consumption. The Monte Carlo method based on the eigenvectors and eigenvalues of relaxation matrix also seems to be very efficient due to parallelising the computer code. Of course, the CPU time consumption of standard vector algebra algorithms is proportional to N^3, where N is the number of molecules (dimension of investigated matrix). Therefore this method is particularly good when applied to one component systems.

The excellent agreement between the SCDM and MC leads to the conclusion that the theory of interest can be used in description of real physical systems. Further developments taking into account also the effect of direct light absorption by acceptors occurring mostly in real physical systems as well as time - resolved and steady - state experiments are in preparation.

Acknowledgement

References

[1]   A. Kawski, *Photochem. Photobiol.* **38**, 487 (1983).

[2]   C. Bojarski, K. Sienicki, J. F. Rabek (ed.), *Photochemistry and Photophysics,* Vol. 1, CRC Press, Boca Raton, FL, 1 (1989).

[3]   C.R. Gochanour, H.C. Andersen and M.D. Fayer, *J. Chem. Phys.*, **70**, 4254 (1979).

[4]   R.F. Loring, H.C. Andersen and M.D. Fayer, *J. Chem. Phys.*, **76**, 2015 (1982).

[5]   C. Bojarski, *Z. Naturforsch.*, **39a**, 948 (1984).

[6]   C. Bojarski and G. Żurkowska, *Z. Naturforsch.* **42a** , 1451 (1987).

[7]   K. Sienicki and M.A. Winnik, *Chem. Phys.* **121,** 163 (1988).

[8]   R. Twardowski and J. Kuśba, *Z. Naturforch.* **43a** , 627 (1988).

[9]   P. Bojarski, A. Kawski, *J. Fluoresc.*, **2/2**, 133 (1992).

[10] L. Kułak and C. Bojarski, *Chem. Phys.,* **178**, 113 (1993).

[11] L. Kułak and C. Bojarski, *Chem. Phys.* **191**, 43 (1995).

[12] L. Kułak and C. Bojarski, *Chem. Phys.* **191**, 67 (1995).

[13] P. Bojarski and L.Kułak, *Chem.Phys.* (in press)

[14] D. T. Gillespie, *J.Chem. Phys.* **81**, 2340 (1977).

[15] J. Kuśba and R. Twardowski in: *"Międzymolekularne oddziaływania w stanach wzbu-dzonych"*, Ossolineum, 111 (1986) (in Polish).

[16] K. Sienicki, S. Błoński, *J. Phys. Chem.* **95**, 7353 (1991).

[17] K. Sienicki, S. Błoński, and G. Durocher „*J. Phys. Chem.*, **95**, 7353 (1991).

[18] L. Kułak, R. Twardowski, C. Bojarski, J. Appl. Spectroscopy 65 (1995) 177.

[19] P. Bojarski, L.Kulak, C.Bojarski, A.Kawski, J.Fluorescence 5 (1995) 293.